Ab initio characterization of the electronic and optical properties of a new IR nonlinear optical crystal: $K_3V_5O_{14}$

2006 J. Phys.: Condens. Matter 18 5535

(http://iopscience.iop.org/0953-8984/18/23/023)

INSTITUTE OF PHYSICS PUBLISHING JOURNAL OF PHYSICS: CONDENSED MATTER

J. Phys.: Condens. Matter **18** (2006) 5535–5544 doi:10.1088/0953-8984/18/23/023

Ab initio characterization of the electronic and optical properties of a new IR nonlinear optical crystal: $K_3V_5O_{14}$

S-P Huang, D-S Wu, J Shen, W-D Cheng[1], Y-Z Lan, F-F Li, H Zhang and Y-J Gong

State Key Laboratory of Structural Chemistry, Fujian Institute of Research on the Structure of Matter, The Graduate School of the Chinese Academy of Sciences, Fuzhou, Fujian 350002, People's Republic of China

E-mail: cwd@ms.fjirsm.ac.cn

Received 18 January 2006
Published 26 May 2006
Online at stacks.iop.org/JPhysCM/18/5535

Abstract

We present detailed investigations of the electronic and optical properties of $K_3V_5O_{14}$, including the band structure, density of states (DOS), population analysis, dielectric function, refractive index and second-order nonlinear susceptibilities. The calculations are performed using the *ab initio* pseudopotential density functional method combined with an anharmonic oscillator model, in which we employ the Perdew–Burke–Eruzerhof form of the generalized gradient approximation together with plane-wave basis sets for expanding the periodic electron density. From the band calculation, $K_3V_5O_{14}$ is predicted to be an indirect band gap semiconductor. From the DOS and population analysis, we find that the bonding between K^+ and V_5O_{14} layers is mainly ionic while that between V and O is covalent. It is indicated that the hybridization of V-3d with the O-2p states is very important for the optical properties of $K_3V_5O_{14}$. The calculated birefringence is large enough to achieve phase-matchable conditions, and our calculated second-harmonic-generation (SHG) coefficients agree with experimental results.

(Some figures in this article are in colour only in the electronic version)

1. Introduction

The investigation of new optical crystals have become a hotspot of laser science and technology in the past two decades. The crystal $K_3V_5O_{14}$ has recently been verified experimentally to present nonlinear optical properties in the infrared (IR) region [1]. Powder double-frequency

[1] Author to whom any correspondence should be addressed.

0953-8984/06/235535+10$30.00

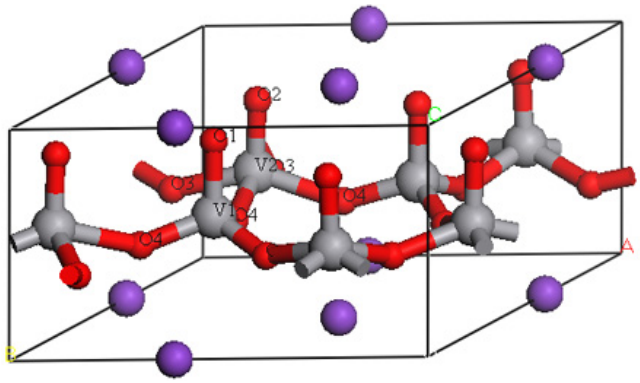

Figure 1. Unit cell of $K_3V_5O_{14}$.

studies show that its SHG signal is about 20 times that of KH_2PO_4 (KDP). Its main transparent range in the IR region is 3–10 μm, and there is another transparent range at 18–21 μm.

There are few reports on the $K_3V_5O_{14}$ crystal. The first synthesis of $K_3V_5O_{14}$ was worked out from aqueous solution by Bystrom and Evans [2]. Kelmers found this phase in a study of the system KVO_3–V_2O_5 [3]. Its single crystal has been grown by cooling melts of K_2CO_3 and V_2O_5, and it has been proposed as a new nonlinear optical material by Li [1].

$K_3V_5O_{14}$ crystallizes into a trigonal structure with space group $P31m$ and lattice constants $a = 8.679\,65$ Å and $c = 4.991\,400$ Å [2]. Figure 1 shows the unit cell of $K_3V_5O_{14}$. There are two and four crystallographically inequivalent sites for V (V1,V2) and O (O1, O2, O3, O4), respectively. V1 is fourfold-coordinated, while V2 is fivefold-coordinated. Five vanadium atoms lie very nearly in the same z-plane, forming almost regular pentagons. The oxygen atoms form nearly square pyramids around the V2 atoms and trigonal pyramids around the V1 atoms; all of the pyramids have apices pointing in the same direction along the c-axis. The V_5O_{14} layers are separated by K^+ ions, which fit equally well on both sides of the layer.

Up to now, there have been no reports of the experimental determination of the energy gap of $K_3V_5O_{14}$. In order to verify our calculated band structure for $K_3V_5O_{14}$, we also calculate the electronic properties of V_2O_5, which belongs to the *Pmmn* space group. In this paper, we will present results of the electronic structure and optical properties of $K_3V_5O_{14}$ calculated by first-principles quantum mechanics combined with an anharmonic oscillator model, and give an understanding of the optical transition for this material.

2. Computational method

2.1. For electronic structures and linear optical properties

All calculations use the total-energy code CASTEP, [4, 5] which employs pseudopotentials to describe electron–ion interactions and represents electronic wavefunctions using a plane-wave basis set [6]. Exchange and correlation effects have been treated separately by Perdew–Burke–Ernzerhof (PBE) [7] and Perdew–Wang (PW91) [8] in the generalized gradient approximation. The interactions between the ionic cores and the electrons are described by the norm-conserving pseudo-potential [9]. Pseudo-atomic calculations are performed for K-$3s^23p^64s^1$, O-$2s^22p^4$, and V-$3d^34s^2$. Considering the balance of computational cost and precision, we choose a cut-off energy of 550 eV and a $3 \times 3 \times 6$ k-point set mesh, which make the separation of reciprocal space less than 0.04 $Å^{-1}$. It is important to include a significant number of empty bands when

calculating optical properties. The exact number that is required will depend on the nature and size of the system under consideration, and 60 empty bands are used in the calculations of optical properties.

The linear response of the system to an external electromagnetic field with a small wave vector is measured through the complex dielectric function, $\varepsilon(\omega)$. $\varepsilon(\omega)$ is connected with the interaction of photons with electrons. The real part and imaginary part of $\varepsilon(\omega)$ are often referred to as $\varepsilon_1(\omega)$ and $\varepsilon_2(\omega)$, respectively. $\varepsilon_2(\omega)$ can be thought of as detailing the real transitions between occupied and unoccupied electronic states. The imaginary part $\varepsilon_2(\omega)$ of the dielectric function $\varepsilon(\omega)$ is given by the equation:

$$\varepsilon_2^{ij}(\omega) = \frac{8\pi^2\hbar^2e^2}{(m^2V)}\sum_k\sum_{\mathrm{cv}}(f_\mathrm{c}-f_\mathrm{v})\frac{p^i_{\mathrm{cv}}(k)\,p^j_{\mathrm{vc}}(k)}{(E^2_{\mathrm{vc}})}\delta[E_{\mathrm{cv}}(k)-\hbar\omega] \tag{1}$$

where $E_{\mathrm{cv}}(k) = E_\mathrm{c}(k) - E_\mathrm{v}(k)$. Here, f_c and f_v represent the Fermi distribution functions of the conduction and valence band. The term $p^i_{\mathrm{cv}}(k)$ denotes the momentum matrix element transition from the energy level c of the conduction band to the level v of the valence band at the kth point in the Brillouin zone (BZ), and V is the volume of the unit cell.

The real part $\varepsilon_1(\omega)$ of the dielectric function $\varepsilon(\omega)$ follows from the Kramer–Kronig relationship. All the other optical constants may be derived from $\varepsilon_1(\omega)$ and $\varepsilon_2(\omega)$ [10, 11]. For example, the refractive index $n(\omega)$ can be calculated using the following expression:

$$n(\omega) = \left(\frac{1}{\sqrt{2}}\right)\left[\sqrt{\varepsilon_1^2(\omega)+\varepsilon_2^2(\omega)}+\varepsilon_1(\omega)\right]^{1/2}. \tag{2}$$

2.2. For nonlinear optical properties

There are many different methods for computing SHG coefficients. Champagne and Bishop [12] reviewed the calculation methods for nonlinear optical properties for the solid state, and Boy [13], Ubachs [14] and Bassani and Lucarini [15] gave the relations between the first- and second-order susceptibilities under the approximation of the anharmonic oscillator model, respectively. Kurtz and Robinson [16] calculated the electro-optical coefficients and the second-harmonic generation coefficients from the linear refractive index n, which can be obtained from the first-order susceptibility. Here we calculate the SHG coefficients of $K_3V_5O_{14}$ by first-principles quantum mechanics combined with an anharmonic oscillator model. This model provides a good description for those cases in which all of the optical frequencies are considerably smaller than the lowest electronic resonance frequency of the material system [13]. Also, it has been applied successfully to studying the nonlinear optical properties of $CsCdBr_3$ and $RbCdI_3{\cdot}H_2O$ crystals below the band edge region [17].

When the dielectric function is obtained from first-principles calculations, the first-order non-resonant susceptibility in the low-frequency region is given by $\chi^{(1)}(\omega)_{ii} = [\varepsilon(\omega)_{ii} - 1]/4\pi$. Furthermore, the second-order non-resonant susceptibility can be expressed in terms of the first-order susceptibilities as follows [13, 17]:

$$\chi^{(2)}_{ijk}(-\omega_3;\omega_1,\omega_2) = F^{(2)}\chi^{(1)}_{ii}(\omega_3)\chi^{(1)}_{jj}(\omega_1)\chi^{(1)}_{kk}(\omega_2) \tag{3}$$

where $F^{(2)} = ma/(N^2e^3)$. Equation (3) is derived from a classical anharmonic oscillator (AHO) model [13], where m and e are the electron mass and charge, respectively, and a is a parameter that characterizes the nonlinearity of the response. The value of a can be obtained from experimental or theoretical estimations. It is noted that N is the number density of unit cells in a crystal, instead of the number density of atoms in a classical AHO model.

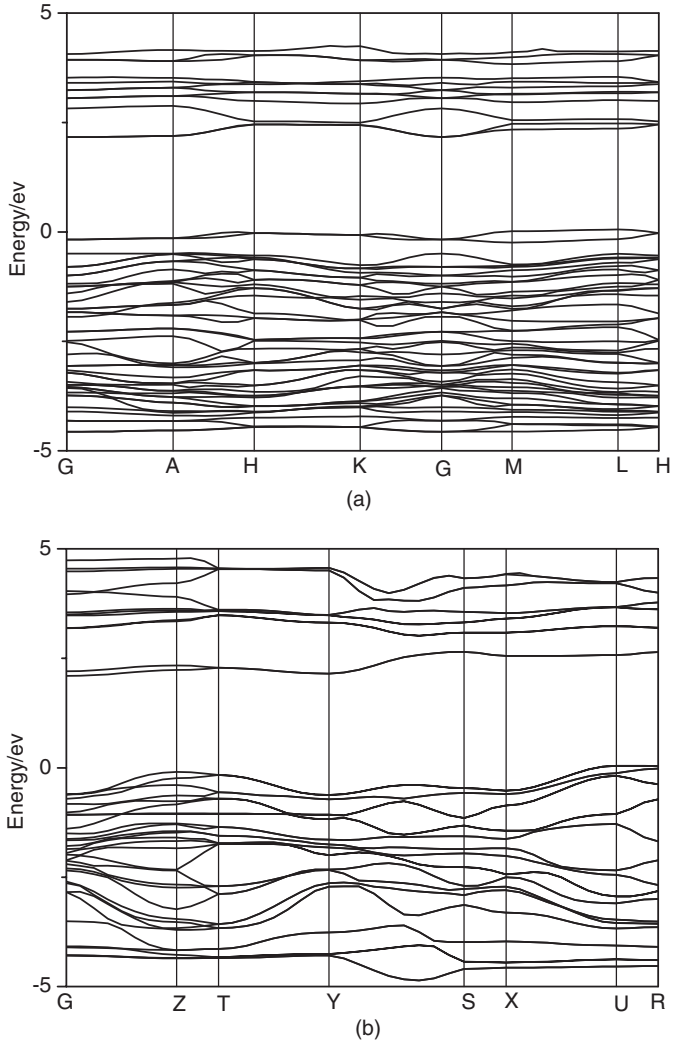

Figure 2. The band structures for the crystals (a) $K_3V_5O_{14}$ and (b) V_2O_5.

3. Results and discussions

The calculations by PBE and PW91 provide very similar electronic structures and optical properties. Here, we only give the plots and the tables calculated by the PBE functional.

3.1. Electronic structure

Figure 2 shows the dispersions of energy bands along the line of high symmetry points in the Brillouin zone. For the sake of clarity, we only show the bands located between −5.0 and 5.0 eV. For V_2O_5, the valence and conduction band are separated by an indirect optical band gap, with the band extrema located at the U (0.0 0.5 0.5) and G(0.0 0.0 0.0) points, respectively. Our calculated size for the indirect gap of 2.10 eV is larger than the calculated value of 1.74 eV of Eyert *et al* [18], and close to the experimental value [19] of 2.3 eV. For $K_3V_5O_{14}$, the top

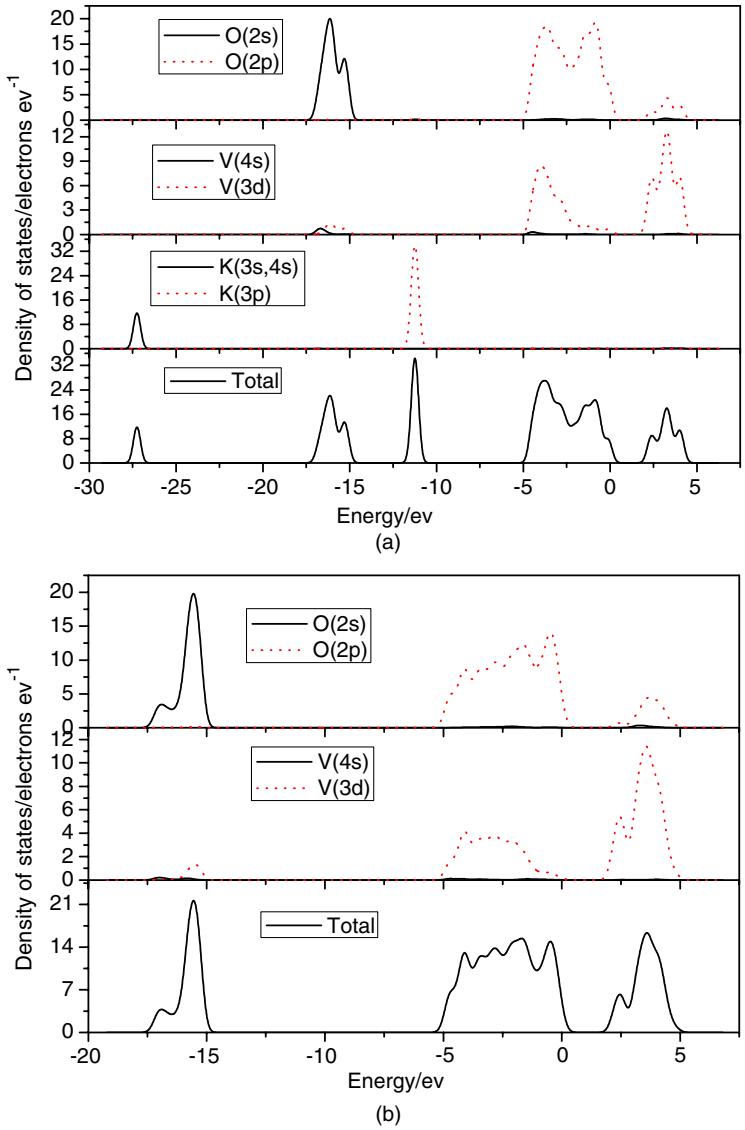

Figure 3. The density of states and partial density of states of (a) $K_3V_5O_{14}$, and (b) V_2O_5.

of the valence bands (VBs) is located at the $L(0.0\ 0.5\ 0.5)$ point, while the bottom of the conduction bands (CBs) is at the $G(0.0\ 0.0\ 0.0)$ point. The calculated indirect gap of $K_3V_5O_{14}$ in PBE is 2.11 eV, and that in PW91 is 2.14 eV. Both the VBs and CBs of $K_3V_5O_{14}$ are denser than those of V_2O_5, because the number of V and O atoms in a unit cell of $K_3V_5O_{14}$ is larger than that for V_2O_5.

The total density of states (DOS) and partial DOS (PDOS) projected on the constitutional atoms are plotted in figure 3. The bands can be assigned according to the total and partial density of states. For $K_3V_5O_{14}$, the regions below the Fermi level (the Fermi level is set at the top of the valence band) contain 68 bands and can be divided into four regions. The bottom-most valence-band region ranging from -27.9 to -26.6 eV is composed of K-3s states. The

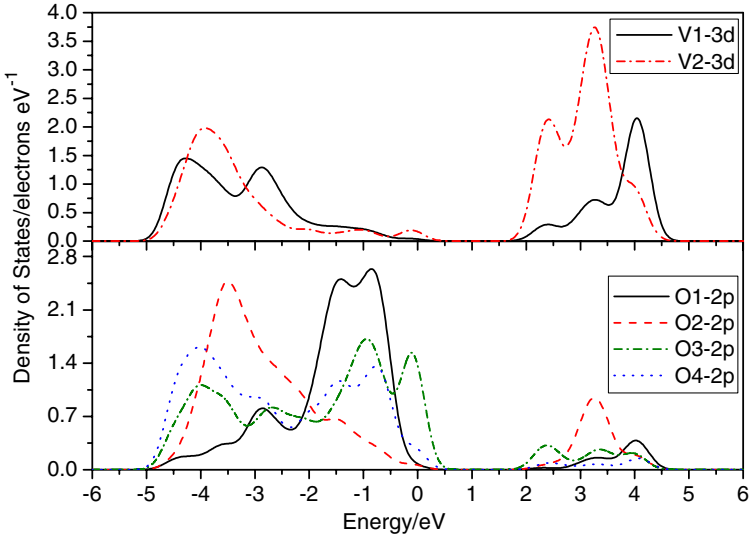

Figure 4. V-3d and O-2p partial DOS of $K_3V_5O_{14}$.

bands ranging from −17.4 to −14.6 eV mostly originate from O-2s states. The K-3p states dominate the bands ranging from −11.9 to −10.5 eV. The top of the valence-band region arises from O-2p states, with a non-negligible contribution from V-3d states. The conduction bands above the Fermi level are mainly due to V-3d states, with a non-negligible contribution from O-2p states. It should be noted that the contribution of the valence electron states of the K atom in $K_3V_5O_{14}$ to the top VBs and bottom CBs is negligible, and both the top VBs and bottom CBs arise from the O-2p and V-3d states for $K_3V_5O_{14}$ and V_2O_5, which make the calculated gaps of $K_3V_5O_{14}$ and V_2O_5 very close. From a comparison of the experimental and theoretical band gaps of V_2O_5, we estimate that the $K_3V_5O_{14}$ indirect band gap is about 2.3 eV.

Figure 4 displays the partial DOS of each type of V and O separately for the top valence bands and the bottom conduction bands. The partial DOSs of O3 and O4 are similar. The shapes of the V1-3d peaks around −4.0 and −2.8 eV resemble those of the O3 and O4 DOSs, and the shapes of the V2-3d peaks around −3.7 and 3.2 eV resembles those of the O2 DOSs. Moreover, the largest DOS (1.45 electrons eV^{-1}) of the V1-3d states are close to those (1.1 and 1.6 electrons eV^{-1}) of the O3-2p and O4-2p states, respectively, and the DOS (2.0 electrons eV^{-1}) of the V2-3d states of around −3.7 eV is near to that (2.4 electrons eV^{-1}) of the O2-2p states. This indicates well-defined p–d hybridizations and V–O covalent interactions. The chemical bonding properties are also evidenced from the population analysis. Table 1 shows the calculated results of Mulliken population analysis. The calculated populations of the V–O bonds are from 0.45 to 1.03 *e*, with an average of 0.78 *e* in a unit cell of $K_3V_5O_{14}$ (covalence single bond order is generally 1.0 *e*). The calculated net charges of O3 and O4 are close, while the charges of O1 and O2 are somewhat different. The net charges of V2 are larger than those of V1, which indicates that a higher coordination number leads to a larger charge. From table 1, it is also seen that the charge transfers from V to O in $K_3V_5O_{14}$ decrease and the bond populations of V–O increase compared with those in V_2O_5. For example, the average net charges of O and V are −0.58 and 0.94 *e*, respectively, and the V–O bond population is 0.78 *e* in $K_3V_5O_{14}$, while those of O and V are −0.57 and 1.40 *e*, and the V–O bond population is 0.61 *e* in V_2O_5. Here, it is noted that, although the

Table 1. Electronic charges of the atoms, bond lengths and bond overlap populations of $K_3V_5O_{14}$ and V_2O_5.

	Charge (e)	Length (Å)	Population
$K_3V_5O_{14}$	O1: −0.59	V1–O1: 1.622	V1–O1: 1.02
	O2: −0.38	V1–O4: 1.653	V1–O4: 0.82
	O3: −0.67	V2–O2: 1.549	V2–O2: 1.03
	O4: −0.69	V2–O3: 1.858	V2–O3: 0.56
	V1: 0.80	V2–O4: 1.932	V2–O4: 0.45
	V2: 1.08		V–O: 0.78 (average)
	K: 1.20		
V_2O_5	V: 1.40		V–O: 0.61
	O: −0.57		

O net charges in $K_3V_5O_{14}$ are almost the same as those in V_2O_5, the V–O bonds have a large population in $K_3V_5O_{14}$. This calculated electronic structure indicates that the hybridization of V-3d with the O-2p states is very important for the optical transition properties of $K_3V_5O_{14}$, and the bonding between K^+ and V_5O_{14} layers is mainly ionic while that between V and O is covalent.

3.2. Optical properties

Further insight into the electronic structure can be obtained by studying the optical properties. The optical functions reflect the fine structure of the energy distribution of the electron states in the valence and conduction bands. In condensed matter systems, there are two contributions to $\varepsilon(\omega)$, namely intraband and interband transitions. The contribution from intraband transitions is important only for metals and electron-deficient compounds. The interband transitions can further be split into direct and indirect transitions. The indirect interband transitions involve the scattering of phonons. It is expected that the indirect transitions give only a small contribution to $\varepsilon(\omega)$ in comparison to the direct transitions [20]. Here, we neglect the indirect transitions.

In figure 5(a), we present our calculated dielectric function for $K_3V_5O_{14}$. The average value of zero-frequency polarized dielectric constants in PBE is $\varepsilon(0) = (\varepsilon_x+\varepsilon_y+\varepsilon_z)/3 = 4.93$, and that in PW91 is 4.89. For trigonal structure, the dielectric functions are resolved into two components: $\varepsilon_{xy}(\omega)$, which is the average of the spectra for polarizations along the x and y directions ($E \perp c$ axis), and $\varepsilon_z(\omega)$, corresponding to the z direction ($E \parallel c$ axis). The anisotropy is especially evident in the highest of the peaks. A certain peak in $\varepsilon_2(\omega)$ could correspond to several direct transitions with the same energy in the band structure. Now we will try to explain the origin of the peaks appearing in the $\varepsilon_2(\omega)$ spectra, based on our electronic structure studies. First, we discuss the case of incident radiation with linear polarization along the x direction. There are three peaks at 2.66, 4.14, and 6.88 eV, respectively, and these are due to the transitions from O-2p to V-3d states. There is an intense peak at about 7.40 eV for linear polarization along the z direction, which mainly comes from the electron transition from O1-2p to V1-3d orbitals. The less intense peak of $\varepsilon_{2z}(\omega)$ at around 23.30 eV is mainly dominated by the transitions from O-2p to V-4s states. The transition between K-3p and O-2p states may lead to the peaks at 9–12 eV for $\varepsilon_{2x}(\omega)$. Comparing the lowest-energy peak of $\varepsilon_{2x}(\omega)$ with that of $\varepsilon_{2z}(\omega)$, we find that the absorption of $K_3V_5O_{14}$ crystal is strongly anisotropic.

The calculated dispersion curve of refractive indices is plotted in figure 5(b). The refractive index n^o is an ordinary refractive index which describes the refraction of light polarized perpendicular to the plane containing the propagation vector k and the optic axis. The refractive

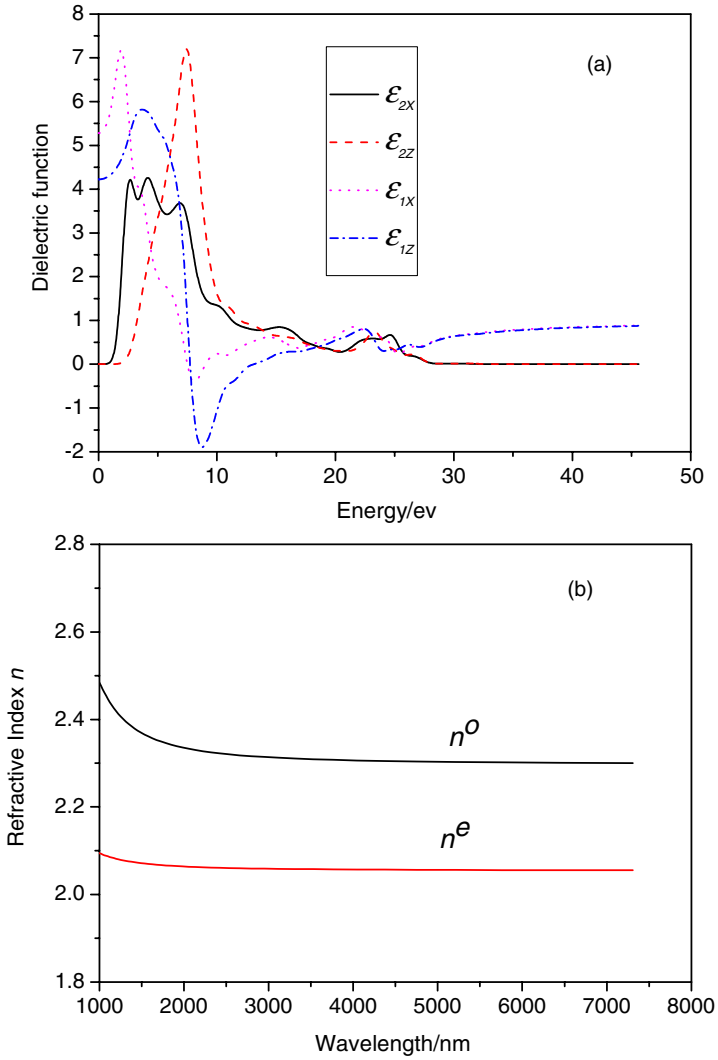

Figure 5. (a) The dielectric function and (b) dispersions of refractive indices of $K_3V_5O_{14}$.

index n^e is an extraordinary refractive index which describes the refraction of light polarized in the plane containing k and the optic axis. From figure 5(b) it can be found that n^o ($n^o = n^a$) is larger than n^e ($n^e = n^c$), and $K_3V_5O_{14}$ is a negative uniaxial crystal. The calculated anisotropic orders of the refractive indices agree well with the result in [2]. The calculated n^o and n^e at a wavelength of 3000 nm are 2.313 and 2.059 respectively, which are a little different from the values of 2.42 and 1.748 in [2]. Also, the calculated birefringence, Δn, at 3000 nm is 0.277, which is large enough to achieve the phase-matchable condition.

$K_3V_5O_{14}$ belongs to the class $31m$ and has 11 nonvanishing tensor elements of second-order susceptibility. Under the restriction of Kleinman's symmetry, there are only three independent components (zzz, yyy, xxz) left. The dynamic susceptibilities $\chi^{(2)}(-2\omega, \omega, \omega)_{ijk}$ are plotted in figure 6. The calculated values of d_{33}, d_{22} and d_{15} ($d = \frac{1}{2}\chi^{(2)}$) are about 1.29×10^{-8}, 3.75×10^{-8} and 2.56×10^{-8} esu, at a wavelength of 1064 nm,

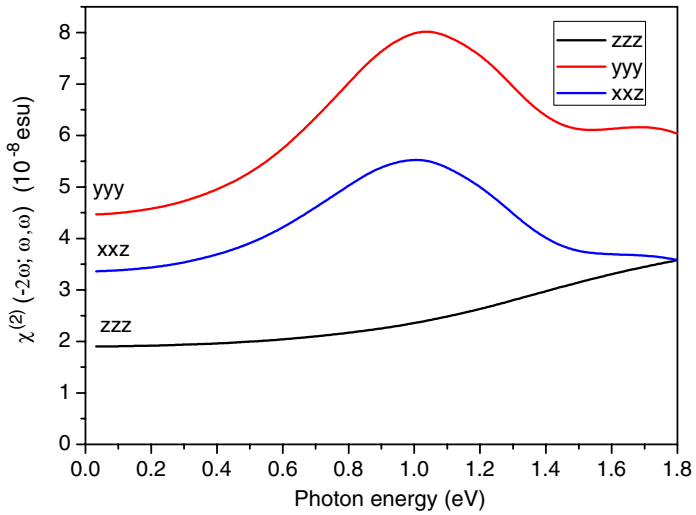

Figure 6. Dynamic second-order optical susceptibilities of $K_3V_5O_{14}$.

respectively. These values are in agreement with the powder double-frequency studies in [1], which showed that the signal for $K_3V_5O_{14}$ was about 20 times to that for KDP ($d_{36} = 1.1 \times 10^{-9}$ esu).

4. Conclusions

A detailed analysis of the electronic structures and optical properties of $K_3V_5O_{14}$ has been performed in view of the results calculated by the DFT method combined with an anharmonic oscillator model. The results that are obtained show that the nature of the fundamental gap in $K_3V_5O_{14}$ is indirect. By comparison between the experimental and theoretical band gaps of V_2O_5, we derive the $K_3V_5O_{14}$ band gap to be close to 2.3 eV. Using the partial density of states and band structure, we have analysed the interband transition contribution to the optical properties for $K_3V_5O_{14}$. The charge transfers from O^{2-} 2p states to V^{5+} 3d states comprise the main contributions to the optical properties of $K_3V_5O_{14}$. The calculated birefringence is large enough to achieve the phase-matchable condition, and our calculated SHG coefficients agree with experimental results.

Acknowledgments

This investigation was based on work supported by the National Basic Research Program of China (No. 2004CB720605), the National Natural Science Foundation of China under projects (20373073 and 90201015), the Science Foundation of the Fujian Province (No. E0210028), and the Foundation of State Key Laboratory of Structural Chemistry (No. 060007).

References

[1] Li G H, Su G B, Zhuang X X, Li Z D and He Y P 2004 *Opt. Mater.* **27** 539
[2] Byström A M and Evans H T Jr 1959 *Acta Chem. Scand.* **13** 377
[3] Kelmers A D 1961 *J. Inorg. Nucl. Chem.* **17** 168

[4] Milman V, Winkler B, White J A, Pickard C J, Payne M C, Akhmatskaya E V and Nobes R H 2000 *Int. J. Quantum Chem.* **77** 895
[5] Segall M D, Lindan P L D, Probert M J, Pickard C J, Hasnip P J, Clark S J and Payne M C 2002 *J. Phys.: Condens. Matter* **14** 2717
[6] Payne M C, Teter M P, Allan D C and Joannopoulos J D 1992 *Rev. Mod. Phys.* **64** 1045 and references therein
[7] Perdew J P, Burke K and Ernzerhof M 1996 *Phys. Rev. Lett.* **77** 3865
[8] Perdew J P, Chevary J A, Vosko S H, Jackson K A, Pederson M R, Singh D J and Fiolhais C 1992 *Phys. Rev.* B **46** 6671
[9] Lin J S, Qteish A, Payne M C and Heine V 1993 *Phys. Rev.* B **47** 4174
[10] Saha S and Sinha T P 2000 *Phys. Rev.* B **62** 8828
[11] Cai M Q, Yin Z and Zhang M S 2003 *Appl. Phys. Lett.* **83** 2805
[12] Champagne B and Bishop D M 2003 *Adv. Chem. Phys.* **126** 41
[13] Boyd R W 1992 *Nonlinear Optics* (New York: Academic) pp 21–32
[14] Ubachs W 2001 *Nonlinear Optics Lecture Notes* Laser Centre Vrije Universiteit Amsterdam, Deparment of Physics and Astronomy, pp 6–10
[15] Bassani F and Lucarini V 1998 *Nuovo Cimento* **20** 1117
[16] Kurts S K and Robinson F N H 1967 *Appl. Phys. Lett.* **10** 62
[17] Huang S P, Cheng W D, Wu D S, Li X D, Lan Y Z, Li F F, Shen J, Zhang H and Gong Y J 2006 *J. Appl. Phys.* **99** 013516
[18] Eyert V and Höck K H 1998 *Phys. Rev.* B **57** 12727
[19] Kenny N, Kannewurf C R and Whitmore D H 1996 *J. Phys. Chem. Solids* **27** 1237
[20] Smith N V 1971 *Phys. Rev.* B **3** 1862